

# Computational Redesign of a PETase for Plastic Biodegradation under Ambient Condition by the GRAPE Strategy

Yinglu Cui, Yanchun Chen, Xinyue Liu, Sajun Dong, Yu'e Tian, Yuxin Qiao, Ruchira Mitra, Jing Han, Chunli Li, Xu Han, Weidong Liu, Quan Chen, Wangqing Wei, Xin Wang, Wenbin Du, Shuangyan Tang, Hua Xiang, Haiyan Liu, Yong Liang, Kendall N. Houk, and Bian Wu\*



Cite This: *ACS Catal.* 2021, 11, 1340–1350



Read Online

ACCESS |

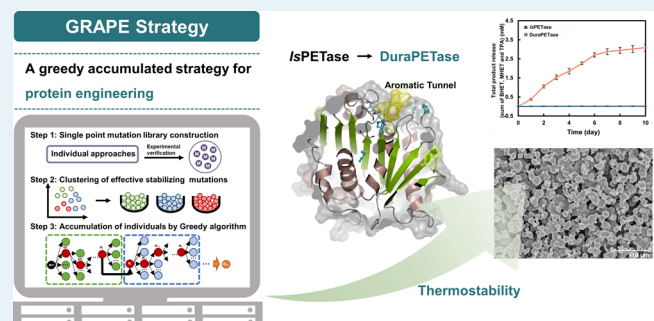
Metrics & More

Article Recommendations

Supporting Information

**ABSTRACT:** Nature has provided a fantastic array of enzymes that are responsible for essential biochemical functions but not usually suitable for technological applications. Not content with the natural repertoire, protein engineering holds promise to extend the applications of improved enzymes with tailored properties. However, engineering of robust proteins remains a difficult task since the positive mutation library may not cooperate to reach the target function in most cases owing to the ubiquity of epistatic effects. The main demand lies in identifying an efficient path of accumulated mutations. Herein, we devised a computational strategy (greedy accumulated strategy for protein engineering, GRAPE) to improve the robustness of a PETase from *Ideonella sakaiensis*. A systematic clustering analysis combined with greedy accumulation of beneficial mutations in a computationally derived library enabled the redesign of a variant, DuraPETase, which exhibits an apparent melting temperature that is drastically elevated by 31 °C and a strikingly enhanced degradation toward semicrystalline poly(ethylene terephthalate) (PET) films (30%) at mild temperatures (over 300-fold). Complete biodegradation of 2 g/L microplastics to water-soluble products under mild conditions is also achieved, opening up opportunities to steer the biological degradation of uncollectable PET waste and further conversion of the resulting monomers to high-value molecules. The crystal structure revealed the individual mutation match with the design model. Concurrently, synergistic effects are captured, while epistatic interactions are alleviated during the accumulation process. We anticipate that our design strategy will provide a broadly applicable strategy for global optimization of enzyme performance.

**KEYWORDS:** computational redesign, thermostability, *IsPETase*, plastic biodegradation, synergistic effects



## INTRODUCTION

High chemo-, regio-, and stereoselectivity features make enzymes extremely superb and fascinating catalysts which confer essential biochemical functions. Harnessing even a fraction of their catalytic power represents an enticing prospect for more sustainable applications, fueling efforts to tailor enzymes with desired physical and catalytic properties. However, new functions with large variations in enzyme sequences were generally found to be more destabilizing or even have unintended effects that lead to misfolding and protein aggregation of the target enzyme.<sup>1,2</sup> Therefore, robust enzymes are highly desirable not only for the industrial requirement but also for their evolvability to accommodate a larger variety of destabilizing mutations.

The high speed of algorithm development has improved our ability to manipulate the structures and functions of biological molecules. Numerous stable proteins have been computationally engineered via diverse approaches.<sup>3</sup> Based on the success achieved by the design of individual stabilizing mutations, hybrid strategies have been developed, which significantly enlarge the

number of predicted stabilizing mutations by combining information from several complementarily different approaches based on evolutionary or energy functions, alleviating the sampling bias by individual approaches.<sup>4,5</sup> These strategies allow to identify stabilizing mutations that would be missed by using only force field or phylogeny approaches as these two methods are often complementary. However, the increased amount of the stabilizing mutants expands an exponentially larger library of the possible combination paths. Within a given library of 21 mutations, there are  $21! \approx 10^{19}$  possible paths and 2,097,130 combined variants linking these single mutations. Current hybrid methods tend to perform a simple stepwise combination

Received: November 23, 2020

Revised: January 4, 2021

Published: January 13, 2021



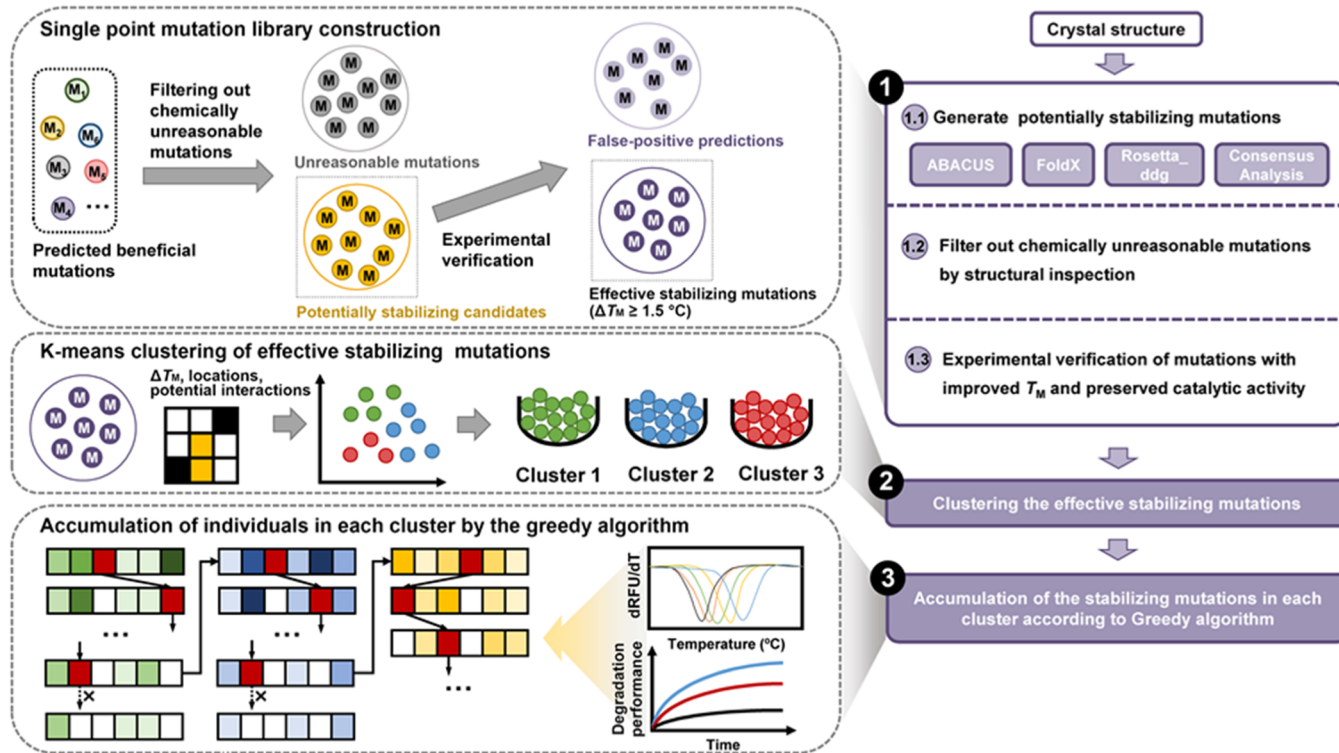


**Figure 1.** Schematic representation of the GRAPE strategy. In step 1, stabilizing mutations are generated with multiple algorithms. The computational designs with typical known pitfalls are eliminated. Then, the remaining designs are selected for experimental validation. Step 2 characterizes the variants according to their positions, efficacies, and presumed effects. Accumulation of the mutations in each cluster according to the greedy algorithm is performed in step 3. Details regarding step 3 are demonstrated in Figure 2.

process to reduce the experimental effort, but in most cases, the combination process fails to immediately find efficient pathways when coupled mutations have negative epistatic interactions.<sup>6,7</sup> The last few years have witnessed impressive progresses in dealing with multidimensional space by a number of metaheuristic methods.<sup>8</sup> Inspired by the widespread greedy algorithm applications in artificial intelligence, we introduce a novel strategy, termed greedy accumulated strategy for protein engineering (GRAPE), to effectively tackle the evolutionary hard problem that enhances the probability of discovering the adaptive routes to improved fitness. To explore the feasibility of this strategy, we performed a proof-of-concept computational engineering of PETase from *Ideonella sakaiensis* 201-F6 (*IsPETase*).

Poly(ethylene terephthalate) (PET) is one of the most widely used man-made synthetic plastics worldwide, with an annual manufacturing capacity of over 30 million tons.<sup>9</sup> Its excellent durability, however, has now become an environmental detriment.<sup>10–12</sup> In the past decade, there have been several foundational studies identifying enzymes that exhibit detectable PET degrading activity.<sup>13–19</sup> Recently, biological recycling of collectable PET materials has been achieved by an engineered thermostable PET hydrolase through thermal and physical pretreatment, contributing toward the concept of a circular PET economy.<sup>19</sup> Although their studies may improve the collectable PET waste disposal practices and recycling capacities, it is still not sufficient to deal with the plastic waste that escape the collection system. Approximately, 40% of plastic waste is not accounted for in managed landfills or recycling facilities annually worldwide and therefore inspires the search for new technologies.<sup>10</sup> Bioremediation is suggested to be an alternative solution,<sup>20</sup> but hydrolysis at elevated temperatures is obviously

incompatible with most bioprocesses using whole-cell catalysts, especially, those involving engineered mesophilic organisms (such as *Escherichia coli*) which can grow up to a maximum temperature of 48–50 °C only after evolutionary adaptation and at a fitness cost.<sup>21</sup> In 2016, *IsPETase* with the highest activity toward amorphous PET at ambient conditions was reported by Yoshida *et al.*,<sup>22</sup> shedding light on the mitigation of the environmental impact of uncollectable PET release beyond current recycling methods.<sup>23–26</sup> However, this enzyme exhibits poor durability: most of its activity is lost within 24 h of incubation at 37 °C.<sup>27</sup> A number of research groups have studied the engineering of *IsPETase*, which has been recently summarized by Taniguchi.<sup>28</sup> Lately reported crystal structures of PET-degrading enzymes allow for methods that exploit rational design to improve the PET degradation performance.<sup>29–35</sup> Successful single-point mutations have afforded 1.2- to 3.1-fold higher activity for PET.<sup>31–36</sup> There is usually a pathway whereby some new functions could be acquired by individually beneficial mutations; however, when the desired function is beyond what a single mutation or double mutations can accomplish, searching in the high-dimensional space involves an incomprehensibly large number of possible pathways among which only an infinitesimal fraction can escape from one local optima trap to reach a better solution.<sup>37</sup>

The proposed GRAPE strategy combines the advantages of greedy and clustering algorithms to provide a viable solution to minimize experimental efforts but maximize the exploration of epistatic effects in terms of additivity and/or synergism between sets of mutations. The redesigned *IsPETase* (DuraPETase) derived from this campaign exhibited an apparent melting temperature increased by 31 °C with good performance toward semicrystalline PET and vastly improved long-term survival

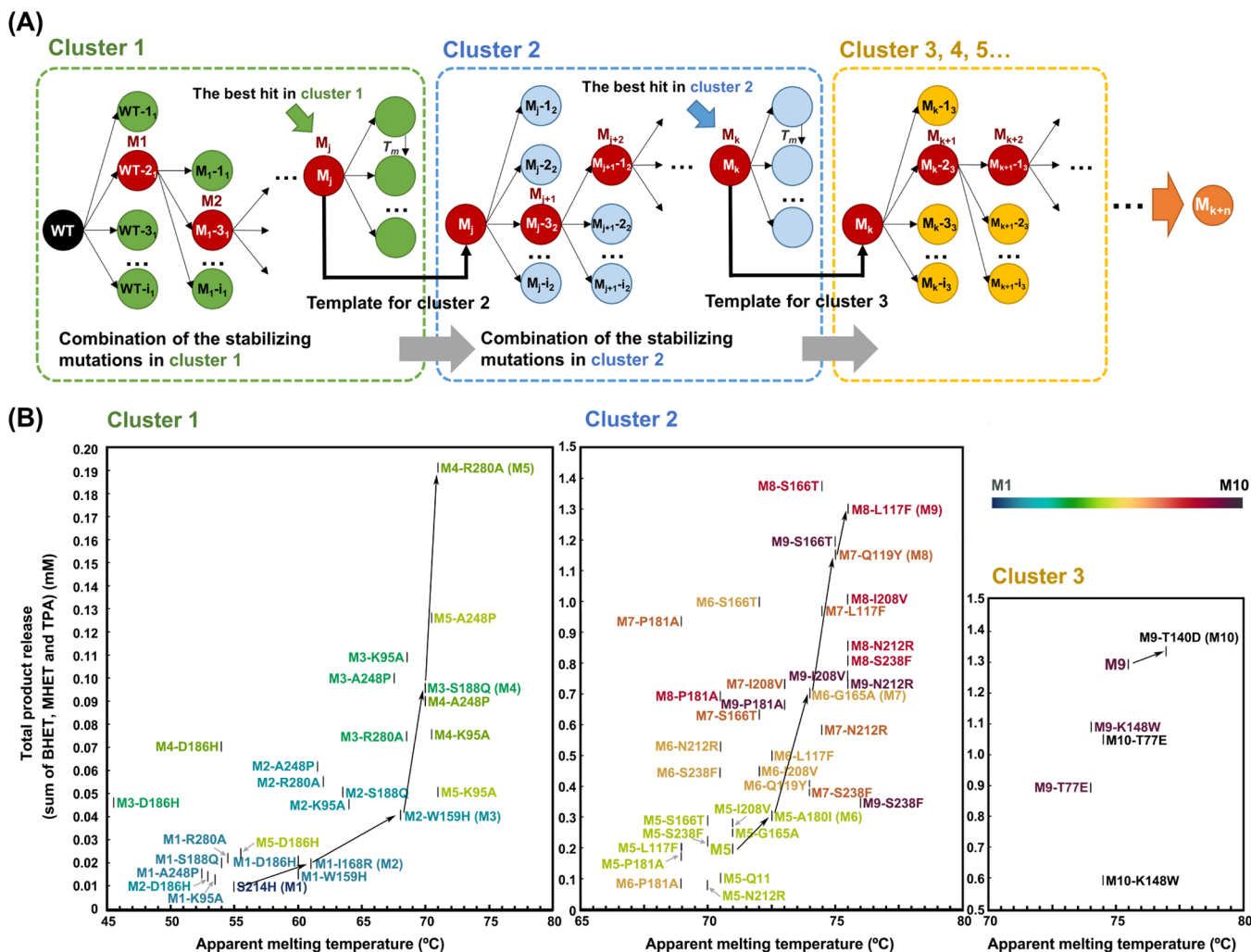


**Figure 2.** (A) Schematic representation of the accumulation step of the mutations in each cluster according to the greedy algorithm. Beneficial mutations in each cluster were crossed with the best hit of the current population until the remaining mutations in the cluster have been traversed or the  $T_m$  values of the combined variants decrease. If the variant showed high thermostability but a degradation reduction of >50%, the combined variant was not adopted. For example, the best hit in cluster 1 ( $M_j$ ) served as the template for further cycles of accumulation in cluster 2, whereas the best hit in cluster 2 ( $M_k$ ) was regarded as the parent for cycles in the next cluster. The best hit in each stage was sequentially referred to as  $M_1, M_2, \dots, M_j, M_{j+1}, \dots, M_k, M_{k+1}, \dots, M_{k+n}$ . The red circles represent the mutants chosen from a combination stage that were used as the template for further accumulation (black arrows). (B) Enhancing the thermostability and degradation performance of *IsPETase* by greedy accumulation. The accumulated mutations in each cluster are listed in Table S4. The introduction of the S187W mutation to the best hit in each round resulted in an extremely decreased expression and thus were not demonstrated in the figure.

under mild conditions. The enzymatic PET degradation was enhanced by over 300-fold at 37 °C for 10 days. Furthermore, complete biodegradation of 2 g/L microplastics to water-soluble products was also achieved. Through this experiment example, we anticipate that the GRAPE strategy will help refine *in silico* enzyme engineering and facilitate its application in cases where improved stabilizing enzymes are required.

## ■ RESULTS

**Computational Redesign of a Robust DuraPETase Using the GRAPE Strategy.** The GRAPE strategy introduced here uses a greedy strategy for global optimization of mutations in each cluster to create functional variations and select the fittest variants to direct the search to higher elevations on the fitness landscape (Figure 1). The initial step in the GRAPE strategy consists of computational predictions of potentially stabilizing mutations along the whole protein sequence. The candidates with typical known pitfalls are eliminated, and the

remaining designs are examined experimentally ([Note S1](#)). Step 2 characterizes the beneficial variants into several clusters according to their positions, efficacies, and presumed effects ([Note S2](#)). This reduces the number of combination paths that need to be screened in the third step. Subsequently, accumulation of the mutations in each cluster according to the greedy algorithm is performed in step 3 to identify an efficient path to achieve the target function ([Note S3](#)).

We previously developed ABACUS<sup>38</sup> software for *de novo* protein design based on a statistical energy function. Here, this algorithm was applied together with three complementary algorithms, FoldX (force field-based energy function),<sup>39</sup> Rosetta\_ddg (force field-based energy function),<sup>40</sup> and Consensus Analysis (phylogeny-based method)<sup>41</sup> to improve the protein stability in the initial step. A total of 253 unique predicted mutations were obtained as potentially stabilizing candidates, among which ABACUS, FoldX, Rosetta\_ddg, and consensus analysis algorithms provided 100, 61, 65, and 54

mutations, respectively, with some overlap. Subsequently, these potentially stabilized candidates were inspected for biophysical pitfalls, such as the introduction of internal cavities, loss of hydrogen-bonding interactions, or exposure of hydrophobic residues at the surface of the enzyme, to improve the quality of the library and reduce the screening effort, providing a sublibrary of 85 candidates. Details are described in the *Supporting Information* (Note S1 and Tables S1–S3). After experimental validation, 21 well-expressed mutants displayed increased stability ( $\geq 1.5$  °C increase in the apparent  $T_m$ ). However, owing to the epistatic effects, these positive mutations may not cooperate to achieve the desired function. Indeed, an *IsPETase* variant containing all 21 beneficial mutations is completely inactive. This restricts the scope for creating stable biocatalysts by stepwise combination alone and calls for knowledge-guided approaches to navigate the combination sequence space.

The GRAPE strategy addresses this challenge by systematically accumulating the beneficial variants in the well-defined library, which is the crucial step for the workflow. The K-means algorithm,<sup>42</sup> which has been proven to be a very powerful tool for data mining problems and has been adopted to perform knowledge discovery in bioinformatics research,<sup>43</sup> was applied to cluster the stabilizing mutations into several groups. The number of clusters in this study was defined as three. Variants were characterized by a set of parameters, including  $\Delta T_m$  improvements, potential effects, interactions between variants, and distances between the  $C\alpha$  atoms of the variants and the catalytic triads. Potential effects caused by the mutations include the introduction of new electrostatic interactions, improvement of hydrophobic packing, and reduction in the conformational entropy. Mutations, which may have interactions (e.g., hydrogen bonds and salt-bridge interactions), were grouped into the same interaction cluster. Details are described in Note S2. Accordingly, the 21 identified stabilizing mutations were clustered into three groups (Table S4), among which K95A, W159H, I168R, D186H, S188Q, S214H, A248P, and R280A were characterized into cluster 1 and L117F, Q119Y, G165A, S166T, A180I, P181A, S187W, I208V, N212R, and S238F were characterized into cluster 2, whereas T77E, T140D, and K148W were clustered into cluster 3.

Subsequently, the best individual of each population served as the parent to attract offspring to its region of the fitness landscape. Each individual in the cluster was crossed with the current global best one. The greedy algorithm accepts the newly generated individual only when its fitness is better than that of the parent. The exploitation process was continued in a multihierarchical manner until all variants in the cluster were traversed or no further improvements were found. Whether a combination stage was positive or deleterious was conditional on the basis of two parameters, that is, thermostability and degradation performance. If the combined variant showed high thermostability but seriously reduced degradation performance, it was advisable to make a compromise. Step 3 in Figure 2A shows the stipulation that each individual stays in its historically best position and moves forward toward the global best position. Details are described in Note S3.

Since new function or adaptive mutations were often found to be more destabilizing, it is advisable to choose stabilized mutants as templates to avoid enzyme unfolding during the accumulation process. Stability-mediated physical features can provide new opportunities for subsequent accumulation, allowing single-point mutations that are neutral or with decreased activity to be non-neutral in the presence of a synergistic interaction.

Therefore, although it exhibited slightly reduced catalytic efficacy, S214 in the first cluster with significantly improved thermostability was considered as the starting point for the initial round of greedy accumulation. Other tasks that want to use the GRAPE strategy to improve the enzyme thermostability are encouraged to choose a more preferred mutation with improved thermostability and enzymatic activity simultaneously. Other mutations in the first cluster (K95A, W159H, I168R, D186H, S188Q, A248P, and R280A) were combined into the S214H mutation and resulted in a best hit (S214H-I168R, M2) in the second stage, which was selected as the new template for next round accumulation (Figure 2B). During the first three stages, the enhanced thermostability may benefit from the newly formed interactions between the mutations and native residues (e.g., new hydrogen-bonding interactions formed between I168R and D186). When S188Q was introduced to M3 (S214H-I168R-W159H), synergistic interactions occurred, leading to the best hit (S214H-I168R-W159H-S188Q, M4) with significantly improved thermostability and degradation performance. In the fifth stage, the introduction of R280A into M4 mainly increased the degradation activity with slight thermostability improvement. However, other mutations combined into M4 even exhibited a reduced  $T_m$  value. Structural analysis suggested that R280A may improve hydrophobic interactions with I232, L249, and I250. Moreover, Kim *et al.*<sup>27</sup> have suggested that the increased activity of R280A was caused by the extended subsite IIc with a nonprotruding cleft. In the sixth stage, it is notable that further introduction of any remaining residues in the first cluster (K95A, D186H, and A248P) failed to increase the  $T_m$  value. Therefore, mutants obtained in the sixth stage were not adopted. After 6 rounds of accumulations, a total of 25 combined mutants were explored experimentally. The best hit (S214H-I168R-W159H-S188Q-R280A, M5) obtained in the first cluster with an increased  $T_m$  value of 71 °C was chosen to be the template for the next crossover of mutations in the second cluster. In the exploitation process of mutations in the second cluster, five rounds of accumulation were performed, and a total of 35 combined mutants were explored. Mutations in the second cluster (L117F, Q119Y, G165A, S166T, A180I, P181A, S187W, I208V, N212R, and S238F) were combined to M5, leading to the best hit (S214H-I168R-W159H-S188Q-R280A-A180I, M6) as the new template. Upon A180I mutation, the extended hydrophobic side chain filled the deep buried hydrophobic core consisting of W97, L101, M157, L199, F201, L230, W257, and M258 to facilitate the interior hydrophobic interactions. In the second stage, the introduction of G165A into M6 enhanced both the degradation activity and thermostability. Structural analysis suggested that the glycine substitution with alanine may stabilize the  $\alpha$ 4 helix, which may further facilitate the stabilization of the catalytic triad. In the third to fourth stages, although the introduction of L117F and Q119Y slightly enhances the  $T_m$  value, significant synergistic interactions were observed when targeting a well-organized hydrophobic domain involving S214H, Trp185, Tyr87, L117F, and Q119Y, resulting in the best hit variant (S214H-I168R-W159H-S188Q-R280A-A180I-G165A-Q119Y-L117F, M9) with vastly improved degradation performance. At the last accumulation stage in the second cluster, the combination of S166T, P181A, I208V, N212R, and S238F to the M9 variant slightly increased the  $T_m$  values but significantly reduced the degradation performance. Therefore, the best hit variant M9 with a  $T_m$  value of 75 °C was considered the template for accumulating mutations in the third cluster. Subsequently,

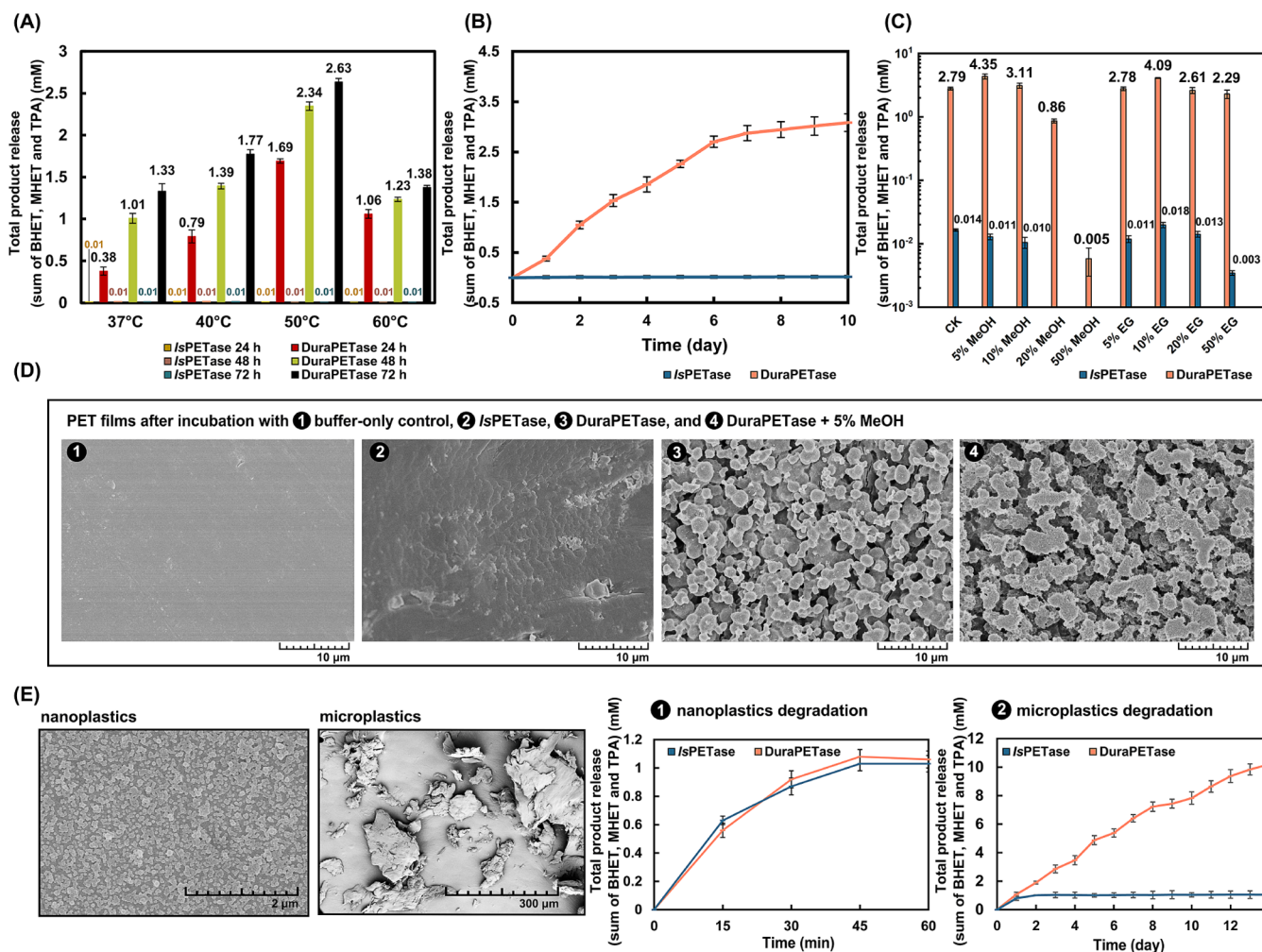


**Figure 3.** (A) Degrading product release of PET film (30% crystallinity) at different temperatures after 3 days of incubation with *IsPETase* and DuraPETase; the enzymes converted PET to TPA and mono(2-hydroxyethyl)-TPA (MHET), with trace amounts of bis(2-hydroxyethyl)-TPA (BHET). The total product release was quantified as the sum of the detected released compounds (TPA, MHET, and BHET). (B) Total product release after incubation with *IsPETase* and DuraPETase for 10 days at 37 °C. (C) Effects of MeOH and EG solvents on the enzymatic degradation of DuraPETase. (D) SEM images for buffer-only PET film control (①), PET films after incubation with *IsPETase* (②), DuraPETase (③) and PET film after incubation with DuraPETase and 5% MeOH (④). All SEM images in (D) were taken after 10 days of incubation at an enzyme loading of 0.01 mg/mL in 50 mM glycine-NaOH buffer (pH 9.0) or with a buffer-only control. (E) SEM image of PET nanoplastics and microplastics before incubation, and hydrolytic performance of DuraPETase toward PET nanoplastics (①) and microplastics (②). PET nanoparticles (200 μL, stock concentration 0.53 g/L) were incubated with 10 μL of enzyme (stock concentration 0.1 mg/mL) in 290 μL of 50 mM glycine-NaOH buffer (pH 9.0) at 37 °C for 1 h. PET microplastics (1 mg) were incubated with 10 μL of enzyme (stock concentration 0.5 mg/mL) in 490 μL of 50 mM glycine-NaOH buffer (pH 9.0) at 37 °C for 2 weeks.

T77E, T140D, and K148W in the third cluster were combined into M9 and resulted in the best hit (S214H-I168R-W159H-S188Q-R280A-A180I-G165A-Q119Y-L117F-T140D, M10) with slightly increased thermostability. Structural analysis suggested that the T140D mutation conferred new hydrogen bonds with the hydroxyl group of Ser142. However, further combination of T77E and K148W into M10 fails to improve both the  $T_m$  value and the degradation activity. Therefore, *IsPETase*-M10 originating from the third cluster (referred to as DuraPETase) was obtained as the most thermostable variant, exhibiting dramatically enhanced thermostability (a  $T_m$  value of 77 °C;  $\Delta T_m = 31$  °C). The greedy accumulation process resulted in a total of 65 combined variants. Progressively addressing the multiple sites in the GRAPE scheme with multilayer upward branches allows negative trade-offs to be determined and quantified and thus finds effective ways to circumvent apparent dead ends. Although the perfect option

along the fitness landscape may not be gained through the limited exploration process, the systematic nature of this strategy maximizes the probability of obtaining cooperative effects of the introduced mutations in a defined region of the fitness landscape within largely reduced experimental efforts. Before addressing the above challenge, we also explored a stepwise combination of the most stabilizing variants ( $\Delta T_m \geq 7$  °C). The stability of the S214H-D186H-I168R mutant was dramatically decreased, and the introduction of the P181A mutation largely reduced the enzymatic degradation.

**Enhanced Degradation Performance toward PET Materials and Other Semiaromatic Polyesters.** With the significantly enhanced properties of DuraPETase, we can explore the anticipated PET digestion of semicrystalline PET film (30%). Given that the biodegradability is strongly affected by the physical properties of PET with different degrees of crystallinity, additives, and surface topology, we selected

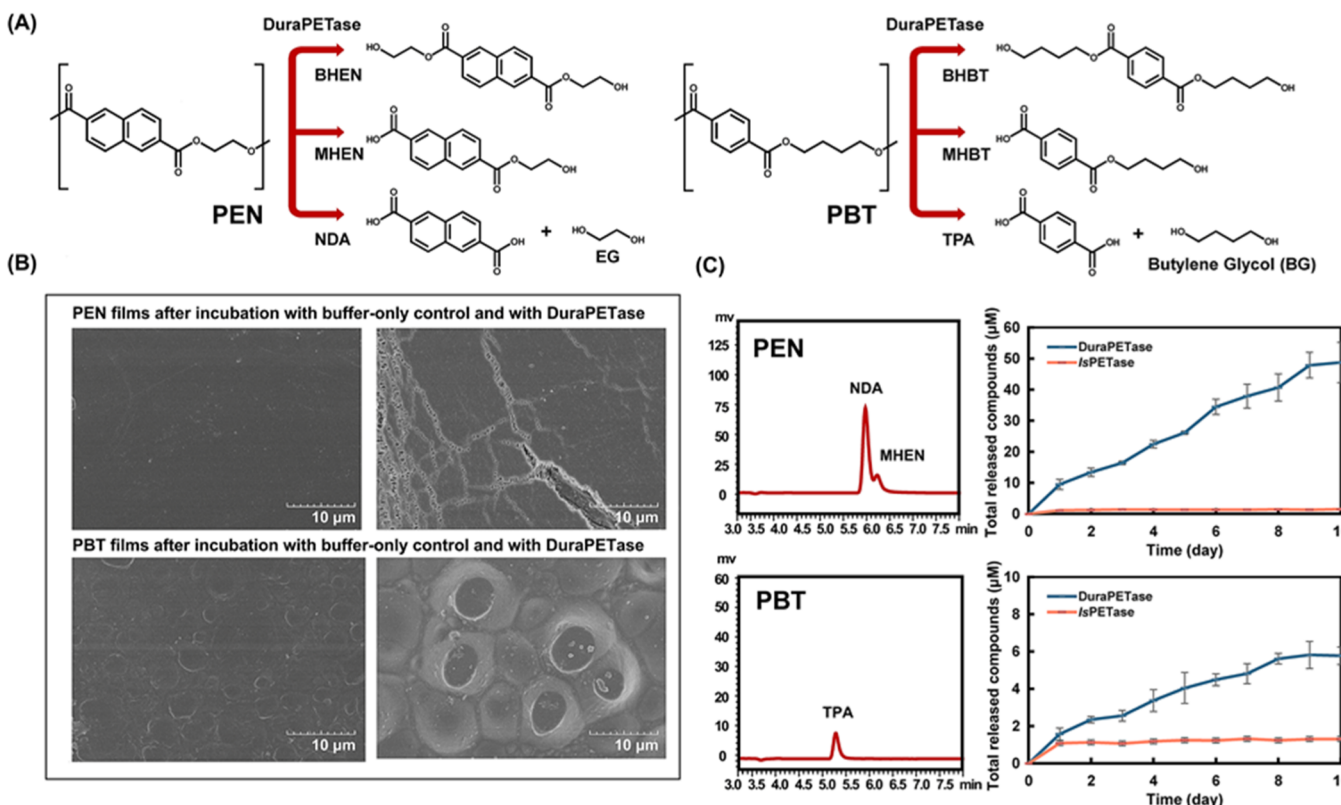


**Figure 4.** (A) PEN and PBT degradation. DuraPETase catalyzes the hydrolytic cleavage of PEN to produce 2,6-naphthalenedicarboxylic acid (NDA), bis(2-hydroxyethyl)-NDA, and mono(2-hydroxyethyl)-NDA and converts PBT to bis(4-hydroxybutyl)-TPA, mono(4-hydroxybutyl)-TPA, and TPA. (B) SEM images of PEN and PBT films after incubation with buffer-only control (left) and with DuraPETase (right). All SEM images were taken after 10 days of incubation at an enzyme loading of 0.01 mg/mL in 50 mM glycine-NaOH buffer (pH 9.0) or with a buffer-only control at 37 °C. (C) HPLC chromatogram of the products released from the PEN and PBT films. Error bars represent s.d. values obtained in triplicate experiments.

common PET materials, which can be easily purchased from Sigma-Aldrich, and further used a simple film preparation process to enable the scientific community to repeat the experiment. The long-term biodegradation performance of DuraPETase was evaluated at 37 °C, which was the optimal temperature for *E. coli* and could further support engineered microorganisms for the downstream conversion of the resulting monomers to high-value molecules.<sup>44</sup> *IsPETase* lost activity within 24 h at 37 °C, and the concentration of the degradation product reached 12  $\mu\text{M}$  and did not increase thereafter, which is consistent with the results in a recent study.<sup>27</sup> As expected, DuraPETase with enhanced thermostability enabled remarkable improvement in long-term survival at moderate temperatures, and the enzyme even withstood elevated temperatures up to 60 °C for 3 days of incubation (Figure 3A). The total released compound concentrations reached up to 3.1 mM when the incubation time was extended to 10 days at 37 °C, which was a 300-fold increase over the concentrations of compounds released by *IsPETase* (Figure 3B). The conversion achieved  $15 \pm 1\%$  by DuraPETase within 10 days. Concomitantly, digestion of PET film with DuraPETase was accompanied by an increase in the crystallinity from 30 to 34% over 10 days (measured by differential scanning calorimetry, Note S4 and Figure S5). Polymer hydrolysis was confirmed by scanning electron microscopy (SEM) images of the film surfaces following enzymatic hydrolysis for 10 days (Figure 3D). Compared to the buffer-only control sample with a smooth and uniform surface, visual modifications with some irregular grooves were observed in *IsPETase*-treated samples. Remark-

ably, severe erosion occurred with the formation of highly porous foam structures on the film surface after 10 days of incubation by DuraPETase, indicating that the hydrolysis behavior was not limited to the hydrolysable polymer end or loops on the polymer surface. We also compared the performance of DuraPETase with several well-characterized PET hydrolases [leaf-branch compost cutinase<sup>15</sup> (LCC), TfH from *Thermobifida fusca*,<sup>13</sup> Tfcut2 from *T. fusca* KW3,<sup>16</sup> Cut190 from *Saccharomonospora viridis* AHK190,<sup>17</sup> and Cut190<sub>Q138A/D250C-E296C/Q123H/N202H</sub>.<sup>18</sup>] The degradation performance of DuraPETase against PET film was 1.7, 13, 55, 10, and 8 times as high as that of LCC, TfH, Tfcut2, Cut190, and Cut190<sub>Q138A/D250C-E296C/Q123H/N202H</sub> after 3 days incubation at 37 °C, respectively, demonstrating the more active degrading ability of DuraPETase than the evaluated PET hydrolases at mild temperatures (Note S4 and Figure S8).

The high degradation performance of DuraPETase allows us to explore whether nanoplastics or even PET microplastics can be completely degraded, which may open new opportunities for wastewater pretreatment. In this work, the total released product determined by high-performance liquid chromatography (HPLC) indicated complete degradation of nanoplastics ( $\phi = 50\text{--}100\text{ nm}$ , 0.21 g/L) by *IsPETase* and DuraPETase within 1 h at 37 °C (Figure 3E), indicating an uncompromising activity of DuraPETase toward substrates even with a largely extended surface dimension. For microplastics degradation, we raised the concentration of PET microplastics to 2 g/L ( $\phi = 0.1\text{--}1\text{ mm}$ , 5 mg of enzyme per gram of PET), which is more than 100-fold higher than in the wastewater treatment plants.<sup>45,46</sup> Although

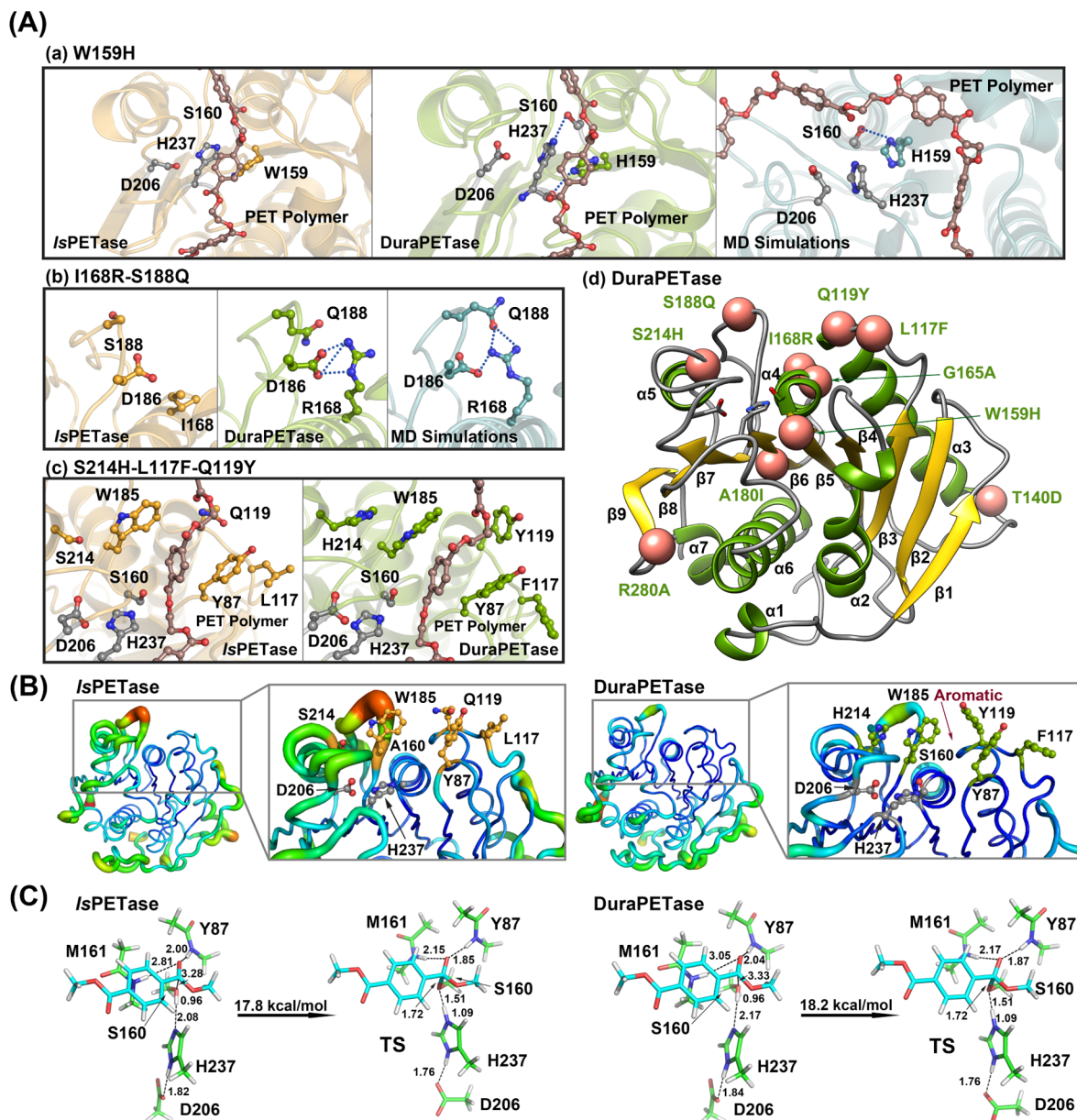


**Figure 5.** Structural features of DuraPETase. (A) Structural effects of (a) W159H, (b) I168R and S188Q, and (c) S214H, L117F, and Q119Y mutations in the DuraPETase crystal structure docked with PET (green) or in MD simulations (blue) compared to those of the *IsPETase* crystal structure docked with PET (bright orange). PET and key residues proximal to the stabilizing mutations are shown in ball and stick representations. The catalytic triad is colored in gray. (d) Location of the stabilizing mutations in the crystal structure of DuraPETase (PDB ID: 6KY5). The DuraPETase structure is shown as a cartoon, while the C $\alpha$  atoms of the stabilizing mutations are shown as coral atoms. (B) B factors of the X-ray structures of *IsPETase* (PDB ID: 5XH3) and DuraPETase, indicating global changes in protein flexibility, especially for the active-site region. (C) DFT-computed activation barriers for *IsPETase* and DuraPETase. The distances are in Å, and the Gibbs free energies are computed with CPCM(water)-B3LYP-D3/6-31+G(d).

much slower degradation of PET microplastics was observed, HPLC analysis of the degradation product concentration reached 9.9 mM, which indicated almost complete degradation of microplastics to water-soluble products by DuraPETase within 2 weeks, contributing toward the concept of microplastic waste treatment in a cost-effective and environmentally friendly manner.

To extend the potential applications of DuraPETase, we also examined the use of this enzyme for the degradation of other semiaromatic polyesters, including polyethylene naphthalate (PEN) and polybutylene terephthalate (PBT) (Figure 4A). Biodegradation of PBT was barely accomplished by *IsPETase*

because of the notably high specificity of the enzyme toward aromatic groups rather than aliphatic chains (Figure 4C). However, a gradual increase in the degradation product release was found for DuraPETase at 37 °C, although the degradation was substantially reduced with respect to the degradation of PET (<1% conversion). SEM analysis also supported this conclusion. In contrast to the slow degradation of PBT, significant enhancement of PEN degradation by DuraPETase was observed. Over 10 days of incubation, DuraPETase produced a maximum product concentration of 48  $\mu$ M with the PEN film, presumably reflecting the high hydrolysis specificity of DuraPETase toward semiaromatic polyesters

because of the redesigned hydrophobic active cleft, even though the degradation activity was still lower than that targeting PET (<1% conversion). As the introduction of the naphthalene ring into the main chain stiffens the polymer chains and largely enhances their dielectric and mechanical properties, PEN holds potential for food packaging, high-performance industrial fiber, and flexible printed circuit applications. Different types of such high-performance plastic would eventually be dispersed into the environment. These results therefore inspire further engineering to improve the depolymerization of new classes of semiaromatic polyesters.

In addition to the broader substrate scope, DuraPETase exhibited a marked increase in tolerance to methanol (MeOH) and ethylene glycol (EG). The degradation was enhanced by 1.6-fold and 1.1-fold at 5 and 10% (v/v) MeOH, respectively, and approximately 30% of degradation ability was maintained at 20% (v/v) MeOH. When incubated with the EG solvent, DuraPETase maintained most of its degradation ability at 5, 20, and 50% (v/v) EG and even increased up to 1.5-fold when incubated with 10% (v/v) EG. The MeOH or EG molecules are suggested to enter between PET chains, weaken hydrogen bonds, and thus increase polymer chain flexibility and accessibility to enzymes. This promoted performance of DuraPETase in cosolvents enhances the potential of this enzyme for auxiliary biodegradation in glycolysis and alcoholysis applications.

**Structural Analysis of the Improved Performance of DuraPETase.** To assess whether the mutations affected the structure as predicted by the design model, we determined the crystal structure of DuraPETase at 1.63 Å resolution (PDB ID: 6KY5), which revealed a conserved  $\alpha/\beta$  hydrolase fold, with a core consisting of seven  $\alpha$ -helices and nine  $\beta$ -sheets. According to the crystal structure and molecular dynamics (MD) simulations, we confirmed a consistent molecular mechanism by which all individual mutations may afford improved stability as the design model proposed. Key aspects were proposed as follows: introduction of new electrostatic interactions (T140D, W159H, I168R, and S188Q), improvement of hydrophobic packing in the protein surface and interior (L117F, Q119Y, A180I, S214H, and R280A), and reduction in the conformational entropy of a local coil region (G165A). Details are described in Note S5. A slight deviation during the MD simulations appeared to be caused by the engineered W159H mutation, which may reconstruct the active site of DuraPETase. The W159H mutation was observed to form a new hydrogen bond with Ser160 for 62.40% in the simulations, resulting in concomitantly flapping of the original catalytic residues His237 and Asp206 out of the catalytic triad (Figure 5A). Similar reconstruction of the catalytic triad was also suggested by Austin *et al.*<sup>31</sup>

One of the major goals in the GRAPE strategy is to minimize the screening requirement and increase the chances of finding cooperative mutations to achieve the desired function. It is noteworthy that the benzene ring of the PET stands at an active-site crevice. Synergistic effects were captured when targeting residues involving S214H, Trp185, Tyr87, L117F, and Q119Y, which we termed as “aromatic tunnel” flanker, to finely tune the active-site cleft suitable for the PET chain. Tyr87, Q119Y, and Trp185 were observed to form continuous  $\pi-\pi$  interactions with the aromatic motif of PET for 52.40, 29.88, and 46.28% of the entire trajectory, respectively. Simultaneously, L117F and Q119Y were located in proximity to the active site and promoted “T-shaped”  $\pi-\pi$  interactions with Tyr87 (the oxyanion hole-

forming residue) for 64.20 and 25.40% of the trajectory, respectively. The stability of the oxyanion hole may be enhanced, and the tetrahedral intermediate can be further stabilized. Another substitution in the active site, S214H, was suggested to prevent the wobbling of Trp185, and it formed an offset parallel  $\pi-\pi$  stacking interaction with Trp185 for 26.44% of the simulation time. Therefore, the crystal structure and MD simulations suggested a well-organized hydrophobic domain suitable for PET binding, and an “induced-fit” arrangement of the active-site cleft may concomitantly occur. A second synergistic interaction obtained by the GRAPE strategy was the I168R-S188Q mutation. In addition to the new salt–bridge interaction formed between I168R and D186, the guanidine group of I168R also donated new hydrogen bonds to the amide oxygen and backbone oxygen atoms of S188Q in the MD simulations for 24.60% of the trajectory. Adding D186H to S214H-I168R-W159H (M3) and S214H-I168R-W159H-S188Q (M4) exhibits highly impaired performance, which confirm the prevailing trend toward negative epistatic interactions when multiple mutations are combined simultaneously.

Incorporation of the stabilizing mutations collectively resulted in a less-flexible state of the global structure of DuraPETase as revealed by the  $C_{\alpha}$  root-mean-square fluctuation (RMSF) results with low fluctuations (Figure S11). Although the flexibility of the active site region has been largely reduced (Figure 5B), there was no significant differences between the activation barriers for *Is*PETase and DuraPETase, inferring that the intrinsic catalytic ability of DuraPETase was not substantially improved (Figures 5C and S12). Unlike enzymes hydrolyzing natural polymers such as polyhydroxyalkanoates or cellulose, the hydrophobic nature of PET represents a barrier which hampers the effective adsorption of enzymes to the polymer surface for the hydrolytic reaction.<sup>11</sup> Specific binding domains responsible for substrate adsorption are absent in *Is*PETase. Therefore, mutation effects, especially by the hydrophobic substitutions, were suggested to enhance the stability as well as the hydrophobic patches toward polymer chains to better accommodate the polymeric substrate, which improve efficient binding and avoid the nonspecific binding of the enzyme to block the contact surface and reduce hydrolysis.<sup>47</sup> However, the mechanism underlying the improved properties of DuraPETase remains elusive, which may be pursued in future efforts through more in-depth research.

## DISCUSSION

Durability, the greatest asset of plastic, has now become a lingering curse that results in plastic remaining in our environment for hundreds of years. Even when physically broken, plastics never truly leave the environment but are present as micro- and nanoplastics that are choking marine life and propagating up the food chain. The biodegradation of plastics under ambient conditions, especially for uncollectable microplastics, is highly desirable to enhance changes in this scenario. To this end, the seminal discovery of *Is*PETase immediately aroused immense interest from numerous research groups in investigating the mechanistic basis of its catalytic mechanism and in increasing the efficiency and stability of this exciting enzyme. Although combining random mutagenesis with high-throughput screening has proven to be a successful strategy for the modification of enzyme properties, a long-sought alternative to screening-based approaches is reliable *in silico* design of performance-enhancing mutations, especially for the

degradation of insoluble solid synthetic polymers.<sup>48–52</sup> Over the last 20 years, *in silico* design based on energy calculations has advanced greatly from fairly simple to increasingly accurate and versatile methods.<sup>4,5</sup> However, the accuracy based on energy functions is still suboptimal because of several factors, including insufficient conformational sampling of the static structure, imbalances in the force fields, and intrinsic problems with existing data sets.<sup>3</sup> Although the drawbacks can be mitigated by using hybrid methods that incorporate complementary statistical-based approaches such as ABACUS, most stability strategies focus on single-point mutation or simple stepwise combination processes, resulting in increased prediction errors upon application to multiple-point mutants. Whenever epistatic effects are present, the predictions are prone to frustrate optimization processes.

The GRAPE strategy proposed in this study represents a step forward in the computational enzyme design because of its capability to reduce the risk of combining mutations with antagonistic effects and independency of the specific structure. A systematic clustering and greedy combination strategy that has been successfully utilized in machine learning therefore provides a way to tap into the possible beneficial pathways in a well-defined library by reducing the dimensionality of the data. The results show that the computational design in combination with experimental screening of <200 variants allowed for the rapid engineering of enzyme variants with a dramatically increased thermostability. The computationally redesigned DuraPETase enzyme described herein has substantially improved degradation performance of *Is*PETase toward semicrystalline PET film and sheds light on its potential use in applications such as surface modification of PET fibers and *in situ* disposal of microplastics. Both the crystal structure and MD simulations suggest an “aromatic tunnel” local structure, which may be responsible for the promoted enzymatic performance, indicating a significant effect of the synergy between various beneficial mutations on stability enhancement and hydrophobic targeting. Moreover, significant potential remains for improving its activity further. This enzyme exhibited higher evolvability through its ability to accommodate a larger variety of new-function mutations, thus providing an exciting platform for additional protein engineering and evolution to increase the degradation efficiency without loss of enzyme level.

In summary, this work shows that a collection of subtle variations identified by *in silico* approaches with minimal experimental screening provides clues regarding how to design a PET hydrolase to improve its incorporation of semicrystalline aromatic polyesters. We believe that the proposed GRAPE strategy constitutes a significant advance in enzyme design methodology that is complementary to traditional computational design strategies, which often focus on exquisitely tuned energy evaluations of single mutations. The variant DuraPETase, designed here by the GRAPE strategy, serves as a useful catalyst for efficient PET degradation at moderate temperatures and opens up avenues for research in decreasing environmental microplastic accumulation. Despite the aforementioned achievements, complete degradation of plastic waste still presents a number of challenges. There is an urgent need for further research such as coupling DuraPETase with downstream enzymes and evolved microorganisms, degrading the terephthalic acid (TPA) and EG products, and the combination of degradation system for potential bioremediation applications.

## ASSOCIATED CONTENT

### SI Supporting Information

The Supporting Information is available free of charge at <https://pubs.acs.org/doi/10.1021/acscatal.0c05126>.

Materials and methods, stabilizing mutation prediction with multiple algorithms, clustering the 21 stabilizing mutations, accumulation of individuals in each cluster by the greedy algorithm, enzymatic degradation of PET films, and structural analysis of DuraPETase ([PDF](#))

## AUTHOR INFORMATION

### Corresponding Author

Bian Wu – CAS Key Laboratory of Microbial Physiological and Metabolic Engineering, State Key Laboratory of Microbial Resources, Institute of Microbiology, Chinese Academy of Sciences, Beijing 100101, China; [orcid.org/0000-0002-6524-2049](https://orcid.org/0000-0002-6524-2049); Email: [wub@im.ac.cn](mailto:wub@im.ac.cn)

### Authors

Yinglu Cui – CAS Key Laboratory of Microbial Physiological and Metabolic Engineering, State Key Laboratory of Microbial Resources, Institute of Microbiology, Chinese Academy of Sciences, Beijing 100101, China

Yanchun Chen – CAS Key Laboratory of Microbial Physiological and Metabolic Engineering, State Key Laboratory of Microbial Resources, Institute of Microbiology, Chinese Academy of Sciences, Beijing 100101, China; University of Chinese Academy of Sciences, Beijing 100049, China

Xinyue Liu – CAS Key Laboratory of Microbial Physiological and Metabolic Engineering, State Key Laboratory of Microbial Resources, Institute of Microbiology, Chinese Academy of Sciences, Beijing 100101, China; School of Life Sciences, Hefei National Laboratory for Physical Sciences at the Microscale, University of Science and Technology of China, Hefei 230052, China

Saijun Dong – CAS Key Laboratory of Microbial Physiological and Metabolic Engineering, State Key Laboratory of Microbial Resources, Institute of Microbiology, Chinese Academy of Sciences, Beijing 100101, China

Yu'e Tian – CAS Key Laboratory of Microbial Physiological and Metabolic Engineering, State Key Laboratory of Microbial Resources, Institute of Microbiology, Chinese Academy of Sciences, Beijing 100101, China

Yuxin Qiao – CAS Key Laboratory of Microbial Physiological and Metabolic Engineering, State Key Laboratory of Microbial Resources, Institute of Microbiology, Chinese Academy of Sciences, Beijing 100101, China

Ruchira Mitra – CAS Key Laboratory of Microbial Physiological and Metabolic Engineering, State Key Laboratory of Microbial Resources, Institute of Microbiology, Chinese Academy of Sciences, Beijing 100101, China; University of Chinese Academy of Sciences, Beijing 100049, China

Jing Han – CAS Key Laboratory of Microbial Physiological and Metabolic Engineering, State Key Laboratory of Microbial Resources, Institute of Microbiology, Chinese Academy of Sciences, Beijing 100101, China; [orcid.org/0000-0002-9207-0238](https://orcid.org/0000-0002-9207-0238)

Chunli Li – CAS Key Laboratory of Microbial Physiological and Metabolic Engineering, State Key Laboratory of Microbial

Resources, Institute of Microbiology, Chinese Academy of Sciences, Beijing 100101, China

Xu Han – Industrial Enzymes National Engineering Laboratory, Tianjin Institute of Industrial Biotechnology, Chinese Academy of Sciences, Tianjin 300308, China

Weidong Liu – Industrial Enzymes National Engineering Laboratory, Tianjin Institute of Industrial Biotechnology, Chinese Academy of Sciences, Tianjin 300308, China

Quan Chen – School of Life Sciences, Hefei National Laboratory for Physical Sciences at the Microscale, University of Science and Technology of China, Hefei 230052, China

Wangqing Wei – State Key Laboratory of Coordination Chemistry, Jiangsu Key Laboratory of Advanced Organic Materials, School of Chemistry and Chemical Engineering, Nanjing University, Nanjing 210023, China

Xin Wang – State Key Laboratory of Coordination Chemistry, Jiangsu Key Laboratory of Advanced Organic Materials, School of Chemistry and Chemical Engineering, Nanjing University, Nanjing 210023, China

Wenbin Du – CAS Key Laboratory of Microbial Physiological and Metabolic Engineering, State Key Laboratory of Microbial Resources, Institute of Microbiology, Chinese Academy of Sciences, Beijing 100101, China;  [orcid.org/0000-0002-7401-1410](https://orcid.org/0000-0002-7401-1410)

Shuangyan Tang – CAS Key Laboratory of Microbial Physiological and Metabolic Engineering, State Key Laboratory of Microbial Resources, Institute of Microbiology, Chinese Academy of Sciences, Beijing 100101, China;  [orcid.org/0000-0002-1056-8690](https://orcid.org/0000-0002-1056-8690)

Hua Xiang – CAS Key Laboratory of Microbial Physiological and Metabolic Engineering, State Key Laboratory of Microbial Resources, Institute of Microbiology, Chinese Academy of Sciences, Beijing 100101, China;  [orcid.org/0000-0003-0369-1225](https://orcid.org/0000-0003-0369-1225)

Haiyan Liu – School of Life Sciences, Hefei National Laboratory for Physical Sciences at the Microscale, University of Science and Technology of China, Hefei 230052, China

Yong Liang – State Key Laboratory of Coordination Chemistry, Jiangsu Key Laboratory of Advanced Organic Materials, School of Chemistry and Chemical Engineering, Nanjing University, Nanjing 210023, China;  [orcid.org/0000-0001-5026-6710](https://orcid.org/0000-0001-5026-6710)

Kendall N. Houk – Department of Chemistry and Biochemistry, University of California, Los Angeles, Los Angeles 90095, California, United States;  [orcid.org/0000-0002-8387-5261](https://orcid.org/0000-0002-8387-5261)

Complete contact information is available at:

<https://pubs.acs.org/10.1021/acscatal.0c05126>

## Author Contributions

Y.L.C. and Y.C.C. contributed equally to this work. B.W. initiated the project. Y.L.C., Q.C., and H.Y.L. performed the prediction of beneficial mutations, Y.L.C., Y.C.C., X.Y.L., S.J.D., Y.E.T., and S.Y.T. performed biochemical and biocatalytic experiments, Y.X.Q., R.M., J.H., C.L.L., W.B.D., and H.X. performed polymer degradation experiments, Y.C.C., X.H., and W.L. determined the crystal structure of DuraPETase, W.Q.W., X.W., Y.L., and K.N.H. conducted the DFT calculations, Y.L.C. and B.W. drafted the manuscript, which was revised and approved by all authors.

## Notes

The authors declare no competing financial interest.

## ACKNOWLEDGMENTS

This work is supported by the National Key R&D Program of China (grant no. 2018YFA0901600), the National Natural Science Foundation of China (grant nos. 31601412, 31822002, and 31961133016), the Beijing Natural Science Foundation (8194074), the Biological Resources Programme (KJF-BRP-017-58), and the Key Research Program of Frontier Sciences (ZDBS-LY-SM014) from the Chinese Academy of Sciences. The authors thank Dr. Wenping Wu and Dr. Wanghui Xu from Novozyme for helpful discussions.

## REFERENCES

- (1) Tokuriki, N.; Tawfik, D. S. Stability Effects of Mutations and Protein Evolvability. *Curr. Opin. Struct. Biol.* **2009**, *19*, 596–604.
- (2) Romero, P. A.; Arnold, F. H. Exploring Protein Fitness Landscapes by Directed Evolution. *Nat. Rev. Mol. Cell Biol.* **2009**, *10*, 866–876.
- (3) Musil, M.; Konegger, H.; Hon, J.; Bednar, D.; Damborsky, J. Computational Design of Stable and Soluble Biocatalysts. *ACS Catal.* **2018**, *9*, 1033–1054.
- (4) Bednar, D.; Beerens, K.; Sebestova, E.; Bendl, J.; Khare, S.; Chaloupkova, R.; Prokop, Z.; Brezovsky, J.; Baker, D.; Damborsky, J. FireProt: Energy-and Evolution-based Computational Design of Thermostable Multiple-point Mutants. *PLoS Comput. Biol.* **2015**, *11*, e1004556.
- (5) Wijma, H. J.; Floor, R. J.; Jekel, P. A.; Baker, D.; Marrink, S. J.; Janssen, D. B. Computationally Designed Libraries for Rapid Enzyme Stabilization. *Protein Eng. Des. Sel.* **2014**, *27*, 49–58.
- (6) Bu, Y.; Cui, Y.; Peng, Y.; Hu, M.; Tian, Y. E.; Tao, Y.; Wu, B. Engineering Improved Thermostability of the GH11 Xylanase from Neocallimastix Patriciarum via Computational Library Design. *Appl. Microbiol. Biotechnol.* **2018**, *102*, 3675–3685.
- (7) Mu, Q.; Cui, Y.; Tian, Y. E.; Hu, M.; Tao, Y.; Wu, B. Thermostability Improvement of the Glucose Oxidase from Aspergillus Niger for Efficient Gluconic Acid Production via Computational Design. *Int. J. Biol. Macromol.* **2019**, *136*, 1060–1068.
- (8) Sammut, C.; Webb, G. I. *Encyclopedia of Machine Learning and Data Mining*; Springer Publishing Company, Incorporated, 2017.
- (9) Polyethylene Terephthalate (PET): Production, Price, Market and its Properties. Available at <https://www.plasticsinsight.com/resin-intelligence/resin-prices/polyethylene-terephthalate/> (accessed Dec 26, 2020).
- (10) Worm, B.; Lotze, H. K.; Jubinville, I.; Wilcox, C.; Jambeck, J. Plastic as a Persistent Marine Pollutant. *Annu. Rev. Environ. Resour.* **2017**, *42*, 1–26.
- (11) Wei, R.; Zimmermann, W. Microbial Enzymes for the Recycling of Recalcitrant Petroleum-based Plastics: How Far Are We? *Microb. Biotechnol.* **2017**, *10*, 1308–1322.
- (12) Wei, R.; Zimmermann, W. Biocatalysis as a Green Route for Recycling the Recalcitrant Plastic Polyethylene Terephthalate. *Microb. Biotechnol.* **2017**, *10*, 1302–1307.
- (13) Müller, R.-J.; Schrader, H.; Profe, J.; Dresler, K.; Deckwer, W.-D. Enzymatic Degradation of Poly(Ethylene Terephthalate): Rapid Hydrolyse Using a Hydrolase from *T. fusca*. *Macromol. Rapid Commun.* **2005**, *26*, 1400–1405.
- (14) Ronkvist, Å. M.; Xie, W.; Lu, W.; Gross, R. A. Cutinase-catalyzed Hydrolysis of Poly(Ethylene Terephthalate). *Macromolecules* **2009**, *42*, 5128–5138.
- (15) Sulaiman, S.; Yamato, S.; Kanaya, E.; Kim, J.-J.; Koga, Y.; Takano, K.; Kanaya, S. Isolation of a Novel Cutinase Homology with Polyethylene Terephthalate-degrading Activity from Leaf-branch Compost by Using a Metagenomic Approach. *Appl. Environ. Microbiol.* **2012**, *78*, 1556–1562.
- (16) Then, J.; Wei, R.; Oeser, T.; Barth, M.; Belisário-Ferrari, M. R.; Schmidt, J.; Zimmermann, W. Ca<sup>2+</sup> and Mg<sup>2+</sup> Binding Site Engineering Increases the Degradation of Polyethylene Terephthalate Films by Polyester Hydrolases from *Thermobifida fusca*. *Biotechnol. J.* **2015**, *10*, 592–598.

- (17) Kawai, F.; Oda, M.; Tamashiro, T.; Waku, T.; Tanaka, N.; Yamamoto, M.; Mizushima, H.; Miyakawa, T.; Tanokura, M. A Novel  $\text{Ca}^{2+}$ -activated, Thermostabilized Polyesterase Capable of Hydrolyzing Polyethylene Terephthalate from *Saccharomonospora Viridis* AHK190. *Appl. Microbiol. Biotechnol.* **2014**, *98*, 10053–10064.
- (18) Oda, M.; Yamagami, Y.; Inaba, S.; Oida, T.; Yamamoto, M.; Kitajima, S.; Kawai, F. Enzymatic Hydrolysis of PET: Functional Roles of Three  $\text{Ca}^{2+}$  Ions Bound to a Cutinase-like Enzyme, Cut190\*, and its Engineering for Improved Activity. *Appl. Microbiol. Biotechnol.* **2018**, *102*, 10067–10077.
- (19) Tournier, V.; Topham, C. M.; Gilles, A.; David, B.; Folgoas, C.; Moya-Leclair, E.; Kamionka, E.; Desrousseaux, M.-L.; Texier, H.; Gavalda, S.; Cot, M.; Guémard, E.; Dalibey, M.; Nomme, J.; Cioci, G.; Barbe, S.; Chateau, M.; André, I.; Duquesne, S.; Marty, A. An Engineered PET Depolymerase to Break Down and Recycle Plastic Bottles. *Nature* **2020**, *580*, 216–219.
- (20) Hiraga, K.; Taniguchi, I.; Yoshida, S.; Kimura, Y.; Oda, K. Biodegradation of Waste PET. *EMBO Rep.* **2019**, *20*, e49365.
- (21) Salvador, M.; Abdulmutalib, U.; Gonzalez, J.; Kim, J.; Smith, A. A.; Faulon, J.-L.; Wei, R.; Zimmermann, W.; Jimenez, J. I. Microbial Genes for a Circular and Sustainable Bio-PET Economy. *Genes* **2019**, *10*, 373.
- (22) Yoshida, S.; Hiraga, K.; Takehana, T.; Taniguchi, I.; Yamaji, H.; Maeda, Y.; Toyohara, K.; Miyamoto, K.; Kimura, Y.; Oda, K. A Bacterium that Degrades and Assimilates Poly(Ethylene Terephthalate). *Science* **2016**, *351*, 1196–1199.
- (23) Gewert, B.; Plassmann, M. M.; Macleod, M. Pathways for Degradation of Plastic Polymers Floating in the Marine Environment. *Environ. Sci.: Processes Impacts* **2015**, *17*, 1513–1521.
- (24) Jia, X.; Qin, C.; Friedberger, T.; Guan, Z.; Huang, Z. Efficient and Selective Degradation of Polyethylenes into Liquid Fuels and Waxes Under Mild Conditions. *Sci. Adv.* **2016**, *2*, e1501591.
- (25) Satti, S. M.; Shah, A. A.; Auras, R.; Marsh, T. L. Isolation and Characterization of Bacteria Capable of Degrading Poly(Lactic Acid) at Ambient Temperature. *Polym. Degrad. Stab.* **2017**, *144*, 392–400.
- (26) Auta, H. S.; Emenike, C. U.; Fauziah, S. H. Screening of *Bacillus* Strains Isolated from Mangrove Ecosystems in Peninsular Malaysia for Microplastic Degradation. *Environ. Pollut.* **2017**, *231*, 1552–1559.
- (27) Son, H. F.; Cho, I. J.; Joo, S.; Seo, H.; Sagong, H. Y.; Choi, S. Y.; Lee, S. Y.; Kim, K. J. Rational Protein Engineering of Thermo-stable PETase from *Ideonella Sakaiensis* for Highly Efficient PET Degradation. *ACS Catal.* **2019**, *9*, 3519–3526.
- (28) Taniguchi, I.; Yoshida, S.; Hiraga, K.; Miyamoto, K.; Kimura, Y.; Oda, K. Biodegradation of PET: Current Status and Application Aspects. *ACS Catal.* **2019**, *9*, 4089–4105.
- (29) Palm, G. J.; Reisky, L.; Böttcher, D.; Müller, H.; Michels, E. A. P.; Walczak, M. C.; Berndt, L.; Weiss, M. S.; Bornscheuer, U. T.; Weber, G. Structure of the Plastic-degrading *Ideonella Sakaiensis* MHETase Bound to a Substrate. *Nat. Commun.* **2019**, *10*, 1717.
- (30) Han, X.; Liu, W.; Huang, J. W.; Ma, J.; Zheng, Y.; Ko, T. P.; Xu, L.; Cheng, Y. S.; Chen, C. C.; Guo, R. T. Structural Insight Into Catalytic Mechanism of PET Hydrolase. *Nat. Commun.* **2017**, *8*, 2106.
- (31) Austin, H. P.; Allen, M. D.; Donohoe, B. S.; Rorrer, N. A.; Kearns, F. L.; Silveira, R. L.; Pollard, B. C.; Dominick, G.; Duman, R.; El Omari, K.; Mykhaylyk, V.; Wagner, A.; Michener, W. E.; Amore, A.; Skaf, M. S.; Crowley, M. F.; Thorne, A. W.; Johnson, C. W.; Woodcock, H. L.; McGeehan, J. E.; Beckham, G. T. Characterization and Engineering of a Plastic-degrading Aromatic Polyesterase. *Proc. Natl. Acad. Sci. U.S.A.* **2018**, *115*, E4350–E4357.
- (32) Joo, S.; Cho, I. J.; Seo, H.; Son, H. F.; Sagong, H. Y.; Shin, T. J.; Choi, S. Y.; Lee, S. Y.; Kim, K. J. Structural Insight into Molecular Mechanism of Poly(ethylene terephthalate) Degradation. *Nat. Commun.* **2018**, *9*, 382.
- (33) Liu, B.; He, L.; Wang, L.; Li, T.; Li, C.; Liu, H.; Luo, Y.; Bao, R. Protein Crystallography and Site-direct Mutagenesis Analysis of the Poly(ethylene terephthalate) Hydrolase PETase from *Ideonella sakaiensis*. *ChemBioChem* **2018**, *19*, 1471–1475.
- (34) Fecker, T.; Galaz-Davison, P.; Engelberger, F.; Narui, Y.; Sotomayor, M.; Parra, L. P.; Ramírez-Sarmiento, C. A. Active Site Flexibility as a Hallmark for Efficient PET Degradation by *I. sakaiensis* PETase. *Biophys. J.* **2018**, *114*, 1302–1312.
- (35) Liu, C.; Shi, C.; Zhu, S.; Wei, R.; Yin, C.-C. Structural and Functional Characterization of Polyethylene Terephthalate Hydrolase from *Ideonella sakaiensis*. *Biochem. Biophys. Res. Commun.* **2019**, *508*, 289–294.
- (36) Ma, Y.; Yao, M.; Li, B.; Ding, M.; He, B.; Chen, S.; Zhou, X.; Yuan, Y. Enhanced Poly(ethylene terephthalate) Hydrolase Activity by Protein Engineering. *Engineering* **2018**, *4*, 888–893.
- (37) Weinreich, D. M.; Delaney, N. F.; DePristo, M. A.; Hartl, D. L. Darwinian Evolution Can Follow Only Very Few Mutational Paths to Fitter Proteins. *Science* **2006**, *312*, 111–114.
- (38) Xiong, P.; Wang, M.; Zhou, X. Q.; Zhang, T. C.; Zhang, J. H.; Chen, Q.; Liu, H. Y. Protein Design with a Comprehensive Statistical Energy Function and Boosted by Experimental Selection for Foldability. *Nat. Commun.* **2014**, *5*, 5330.
- (39) Guerois, R.; Nielsen, J. E.; Serrano, L. Predicting Changes in the Stability of Proteins and Protein Complexes: A Study of More Than 1000 Mutations. *J. Mol. Biol.* **2002**, *320*, 369–387.
- (40) Kellogg, E. H.; Leaver-Fay, A.; Baker, D. Role of Conformational Sampling in Computing Mutation-induced Changes in Protein Structure and Stability. *Proteins* **2011**, *79*, 830–838.
- (41) Wheeler, T. J.; Clements, J.; Finn, R. D. Skylign: A Tool for Creating Informative, Interactive Logos Representing Sequence Alignments and Profile Hidden Markov Models. *BMC Bioinf.* **2014**, *15*, 7.
- (42) Jain, A. K. Data clustering: 50 Years Beyond K-means. *Pattern Recogn Lett.* **2010**, *31*, 651–666.
- (43) Quackenbush, J. Computational Analysis of Microarray Data. *Nat. Rev. Genet.* **2001**, *2*, 418–427.
- (44) Wei, R.; Tiso, T.; Bertling, J.; O'Connor, K.; Blank, L. M.; Bornscheuer, U. T. Possibilities and Limitations of Biotechnological Plastic Degradation and Recycling. *Nat. Catal.* **2020**, *3*, 867–871.
- (45) Long, Z.; Pan, Z.; Wang, W.; Ren, J.; Yu, X.; Lin, L.; Lin, H.; Chen, H.; Jin, X. Microplastic Abundance, Characteristics, and Removal in Wastewater Treatment Plants in a Coastal city of China. *Water Res.* **2019**, *155*, 255–265.
- (46) Duis, K.; Coors, A. Microplastics in the Aquatic and Terrestrial Environment: Sources (with a Specific Focus on Personal Care Products), Fate and Effects. *Environ. Sci. Eur.* **2016**, *28*, 2.
- (47) Zimmermann, W.; Billig, S. Enzymes for the Biofunctionalization of Poly(ethylene terephthalate). *Adv. Biochem. Eng./Biotechnol.* **2011**, *125*, 97–120.
- (48) Yang, K. K.; Wu, Z.; Arnold, F. H. Machine-learning-guided Directed Evolution for Protein Engineering. *Nat. Methods* **2019**, *16*, 687–694.
- (49) Sun, Z.; Liu, Q.; Qu, G.; Feng, Y.; Reetz, M. T. Utility of B-factors in Protein Science: Interpreting Rigidity, Flexibility, and Internal Motion and Engineering Thermostability. *Chem. Rev.* **2019**, *119*, 1626–1665.
- (50) Mirts, E. N.; Petrik, I. D.; Hosseinzadeh, P.; Nilges, M. J.; Lu, Y. A Designed Heme-[4Fe-4S] Metalloenzyme Catalyzes Sulfite Reduction Like the Native Enzyme. *Science* **2018**, *361*, 1098–1101.
- (51) Huang, P.-S.; Boyken, S. E.; Baker, D. The Coming of Age of De novo Protein Design. *Nature* **2016**, *537*, 320–327.
- (52) Li, R. F.; Wijma, H. J.; Song, L.; Cui, Y. L.; Otzen, M.; Tian, Y. E.; Du, J. W.; Li, T.; Niu, D. D.; Chen, Y. C.; Feng, J.; Han, J.; Chen, H.; Tao, Y.; Janssen, D. B.; Wu, B. Computational Redesign of Enzymes for Regio- and Enantioselective Hydroamination. *Nat. Chem. Biol.* **2018**, *14*, 664–670.